Exploiting the Potential of Meroterpenoid Cyclases to Expand the Chemical Space of Fungal Meroterpenoids

Takaaki Mitsuhashi,[1,2,‡] Lena Barra,[1,‡] Zachary Powers,[3,‡] Volga Kojasoy,[4,‡] Andrea Cheng,[3] Feng Yang,[3] Yoshimasa Taniguchi,[5] Takashi Kikuchi,[6] Makoto Fujita,[2,7] Dean J. Tantillo,*[,4] John A. Porco, Jr.,*[,3] Ikuro Abe*[,1,8]

[1] Graduate School of Pharmaceutical Sciences, The University of Tokyo, 7-3-1 Hongo, Bunkyo-ku, Tokyo 113-0033, Japan

[2] Division of Advanced Molecular Science, Institute for Molecular Science, National Institutes of Natural Sciences, 5-1 Higashiyama, Myodaiji, Okazaki, 444-8787, Japan

[3] Department of Chemistry and Center for Molecular Discovery (BU-CMD), Boston University, Boston, Massachusetts, 02215, United States

[4] Department of Chemistry, University of California Davis, 1 Shields Avenue, Davis, California 95616, United States

[5] Central Laboratories for Key Technologies, Kirin Holdings Co. Ltd., 1-13-5, Fukuura Kana-zawa-ku, Yokohama-shi, Kanagawa, 236-0004 Japan

[6] Rigaku Corporation, 3-9-12 Matsubara-cho, Akishima-shi, Tokyo 196-8666, Japan

[7] Department of Applied Chemistry, Graduate School of Engineering, The University of Tokyo, 7-3-1 Hongo, Bunkyo-ku, Tokyo 113-8656, Japan

[8] Collaborative Research Institute for Innovative Microbiology, The University of Tokyo, Yayoi 1-1-1, Bunkyo-ku, Tokyo 113-8657, Japan

Meroterpenoids, Meroterpenoid Cyclase, Chemoenzymatic Synthesis, Combinatorial Biosynthesis, Crystalline-Sponge X-Ray Diffraction

ABSTRACT: Fungal meroterpenoids are a diverse group of hybrid natural products with impressive structural complexity and high potential as drug candidates. In this work, we evaluate the promiscuity of the early structure diversity-generating step in fungal meroterpenoid biosynthetic pathways: the multibond-forming polyene cyclizations catalyzed by the yet poorly understood family of fungal meroterpenoid cyclases. In total, 12 unnatural meroterpenoids were accessed chemoenzymatically using synthetic substrates. Their complex structures were determined by 2D NMR studies as well as crystalline-sponge-based X-ray diffraction analyses. The results obtained revealed a high degree of enzyme promiscuity and experimental results which together with quantum chemical calculations provided a deeper insight into the catalytic activity of this new family of non-canonical terpene cyclases. The knowledge obtained paves the way to design and engineer artificial pathways towards second generation meroterpenoids with valuable bioactivities based on combinatorial biosynthetic strategies.

Introduction

Fungal meroterpenoids have earned significant interest from the scientific community as well as from the pharmaceutical and chemical industry due to their remarkable structural architectures and potent bioactivities.[1] Pyripyropene A (**1**), isolated from *Aspergillus fumigatus*, is the strongest known inhibitor of acyl-CoA:cholesterol *acyltransferase* and is being developed for the treatment of atherosclerosis.[2] Additionally, **1** exhibits insecticidal properties and a commercial insecticide based on the pyripyropene core structure has been recently marketed.[3] Derivatives of mycophenolic acid (**2**), isolated from *Penicillium* sp., are clinically used immunosuppressant drugs and inhibit inosine 5'-monophosphate dehydrogenase.[4] Andrastin A (**3**) from *Penicillium albocoremium* is an inhibitor of protein farnesyl transferase and a potent anti-cancer agent,[5] whereas tropolactone D (**4**) from *Aspergillus* sp. is a cytotoxic agent against human colon carcinoma (Figure 1A).[6] The genetic basis for fungal meroterpenoid biosynthesis has only been elucidated in recent years, with the first biosynthetic gene cluster reported for pyripyropene A in 2010.[7] Since then, the discovery of several related gene clusters revealed a common modular assembly logic for all meroterpenoid pathways, composed of i) building block generation (polyketide synthase, oligoprenyl synthase), ii) assembly of building blocks (prenyltransferase), iii) early structural diversification by the action of a novel family of terpene cyclases in tandem with an epoxidase and iv) late stage diversification by tailoring enzymes such as cytochrome P450 monooxygenases and α-ketoglutarate-dependent dioxygenases.[8] Their strong biological activities as well as the conserved modular logic of their biosynthetic pathways make meroterpenoids attractive targets for artificial

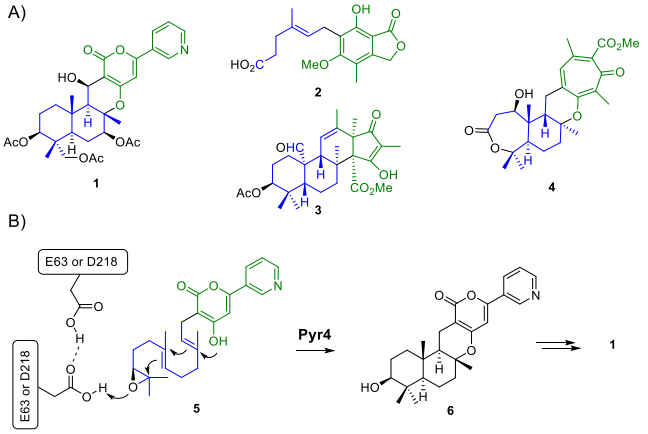

Figure 1. A) Selected examples of fungal meroterpenoids. B) Proposed catalytic mechanism of meroterpenoid cyclases exemplified by Pyr4-mediated reaction of epoxyfarnesyl-HPPO (5) to deacetyl pyripyropene E (6). The polyketide portion is shown in green, terpenoid in blue.

pathway engineering to generate novel structures with new or improved activities. Herein, we set out to evaluate the potential of meroterpenoid cyclases to generate novel scaffolds by employing natural and unnatural synthetic substrate analogues. The results obtained can provide valuable information on matching pathway combinations regarding the interchangeability of employed meroterpenoid cyclases. At the same time, chemoenzymatic access to eight new scaffolds, thus far unprecedented from natural sources or chemical, biomimetic polyene cyclizations, could be achieved.

Results and Discussion

Synthesis of Substrates and Targeted Enzymes

Non-canonical terpene cyclases involved in meroterpenoid biosynthesis are integral membrane proteins of compact size (*ca.* 25 kDa).[7,8] Mutagenesis studies on the model cyclase Pyr4 involved in the pyripyropene biogenesis revealed two highly conserved acidic amino acid residues (Glu63 and Asp218) crucial for enzyme function and proposed to initiate polyene cyclization by protonation of the priorly introduced terminal epoxide function in the prenyl chain, triggering the subsequent polyene cyclization (Figure 1B). The mechanism resembles that of type-II terpene synthases of the 2,3-oxidosqualene-lanosterol cyclase type; however, protein structural data to evaluate the mechanism of meroterpenoid cyclases is still lacking.[7-9] Phylogenetic analysis of characterized meroterpenoid cyclases shows a close relation to the group of Pyr4-like synthases involved in fungal indole diterpene biosynthesis (LtmB, AtmB, and PaxB) and a distant relation to the bacterial enzymes XiaH and DmtA1 (Figure 2).[10]

The substrates of known meroterpenoid cyclases are composed of a linear epoxyoligoprenyl chain, in most cases derived from farnesyl diphosphate (FPP) and a distinct non-terpenoid portion usually generated by a designated polyketide synthase (Figure 2).

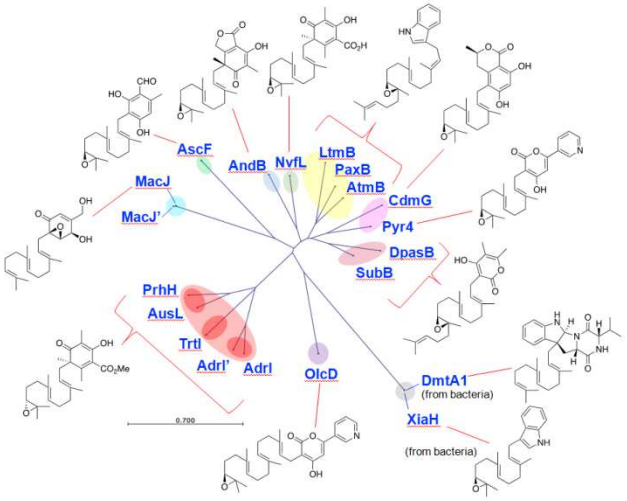

Figure 2. Phylogenetic analysis of reported meroterpenoid cyclases and their respective native substrates.

These biosynthetic intermediates are difficult to obtain from the natural producer, since typically low concentrations are observed and the frequently employed heterologous expression host *Aspergillus oryzae* contains endogenous hydrolases producing high amounts of a shunt diol product.[7] To overcome this limitation, we recently developed a modular synthesis of the widespread 3,5-dimethylorsellinic acid (DMOA)-containing substrate family. The methodology involves base-mediated, regioselective dearomatization of DMOA with farnesyl electrophiles.[11] We expanded the synthetic scope by employing enantiopure (10*R*)- and (10*S*)-epoxyfarnesyl building blocks in this reaction to obtain the naturally occurring substrate (10*R*)- and (10*S*)-(2*E*,6*E*)-5'-DMOA methylester (**7a**, **7b**), as well as (10*R*)- and (10*S*)-(2*E*,6*E*)-3'-DMOA methylester (**8a**, **8b**). Additionally, we also accessed the (2*Z*,6*E*)-epoxyfarnesyl congeners (10*R*)- and (10*S*)-(2*Z*,6*E*)-5'-DMOA methylester (**9a**, **9b**) and (10*R*)- and (10*S*)-(2*Z*,6*E*)-3'-DMOA methylester (**10a**, **10b**) using the same strategy (Figure S1, Figure 3). As dearomative alkylation of DMOA leads to formation of two inseparable diastereoisomers with respect to 3' and 5' ring substitution, the substrates obtained were used as diastereomeric mixtures, exhibiting fixed stereochemistry for the epoxide moiety (88% – 98% *ee*). With substrates in hand, we targeted nine reported meroterpenoid cyclases: Pyr4[7], CdmG[12], AndB[13], AdrI' [14], NvfL[15], PrhH[16], Trt1[17], AscF,[18] and MacJ[19]. As we did not gain access to the MacJ producer strain, we cloned the homologous protein MacJ' from *Penicillium chrysogenum* MT-12 (96% identity). The intron-free genes were expressed in the heterologous host *Saccharomyces cerevisiae* INVSc1 and cell free extracts were prepared and utilized for *in vitro* reactions with synthetic substrates **7a/7b** – **10a/10b**. Monitoring of the reactions by HPLC revealed a surprisingly high degree of promiscuity as several new products were detected (Figure S2-S5, Table 1).

Substrate Scope of Pyr4 and MacJ'

Pyr4, a cyclase which naturally utilizes the (10*S*)-configured epoxide **5** (Figure 1B), was found to accept (10*S*)-(2*E*,6*E*)-5'-DMOA (**7a**), (10*S*)-(2*E*,6*E*)-3'-DMOA (**8a**) as well as

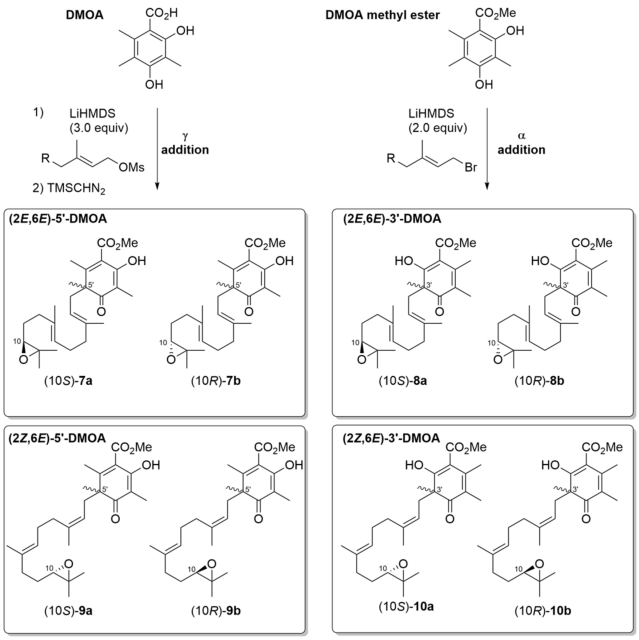

Figure 3. Synthetic approach and structures of obtained and tested DMOA substrates (7a/7b – 10a/10b).

Table 1. Overview on productive enzyme substrate combinations.

	(2*E*,6*E*)-5'-DMOA	(2*E*,6*E*)-3'-DMOA	(2*Z*,6*E*)-5'-DMOA	(2*Z*,6*E*)-3'-DMOA
Pyr4	(10*S*)-**7a**	(10*S*)-**8a**	-	(10*S*)-**10a**
MacJ'	(10*S*)-**7a**	(10*S*)-**8a**	-	(10*S*)-**10a**
CdmG	(10*S*)-**7a**	(10*S*)-**8a**	(10*S*)-**9a**	(10*S*)-**10a**
AndB	(10*S*)-**7a**	(10*S*)-**8a**	(10*S*)-**9a**	-
Trt1	(10*S*)-**7a** (10*R*)-**7b**[a]	-	(10*R*)-**9b**	-
AdrI'	(10*S*)-**7a** (10*R*)-**7b**[a]	-	(10*R*)-**9b**	-
PrhH	(10*R*)-**7b**[a]	-	-	-
NvfL	-	-	-	-
AscF	-	-	-	(10*S*)-**10a**

[a] Native enzyme substrate combination.

(10*S*)-(2*Z*,6*E*)-3'-DMOA (**10a**) based on the detection of newly formed peaks in the HPLC chromatogram (Table 1, Figure S2-S5). To elucidate the structures of the putative new enzyme products, we carried out large scale enzyme preparations in which case reaction of Pyr4 with substrate **7a** led to the isolation of compounds **11** and **12** (Scheme 1A).

Both products exhibit a chair-chair conformation for the A/B ring system, as is also found for the natural cyclization to form pyripyropene E (**6**). However, the terminating cation-quenching step differs for both products, leading to **11** after C-O bond formation and **12** after C-C bond formation. These products were also recently identified from chemical cyclization of *rac*-**7** by using $EtAlCl_2$/Et_2AlCl as Lewis acid promoter.[11] The [3.3.1] bridged structure in **12** is also found in asperterpenes A and B,

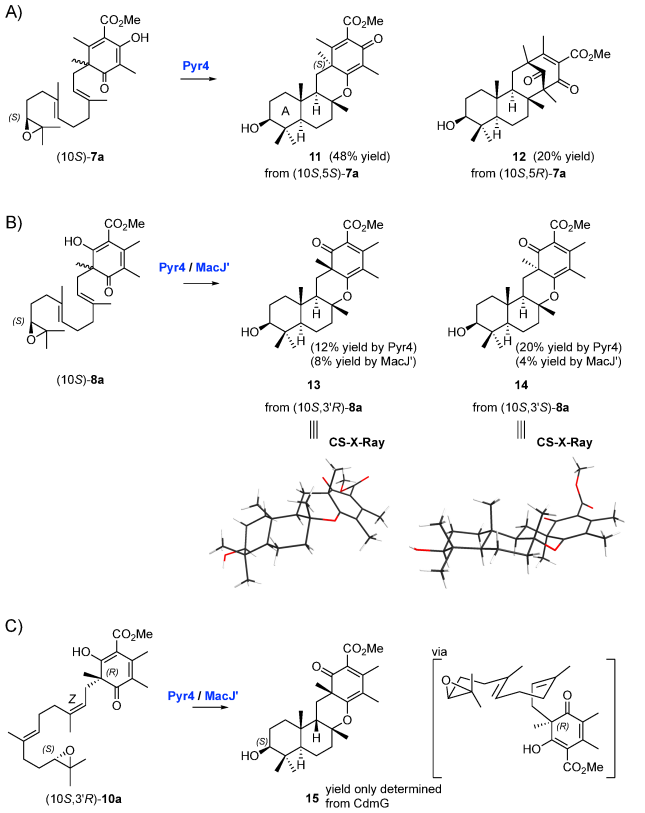

Scheme 1. Structures of isolated meroterpenoids obtained from Pyr4- and MacJ'-mediated reactions with A) (10*S*)-**7a**; B) (10*S*)-**8a**; C) (10*S*,3'*R*)-**10a**.

recently isolated and potent BACE1 inhibitors from *Aspergillus terreus*.[20]

As can be delineated from the configuration of position 5', Pyr4 is able to accept both stereoisomers, (10*S*,5'*S*)-**7a** and (10*S*,5'*R*)-**7a**, to form **11** and **12**, respectively. The findings suggest that Pyr4, which usually accepts the bulkier substrate **5**, exhibits some degree of promiscuity towards changes in the polyketide portion. This is further demonstrated by the successful conversion of (10*S*,3'*R*)-**8a** to **13**, as well as (10*S*,3'*S*)-**8a** to **14**. Substrate **8a** carries the epoxyfarnesyl chain connected to the 3'-position of the DMOA-building block instead of the 5'-position as found in **7a**. Products **13** and **14** also accessed from chair-chair substrate conformations, consistent with the natural substrate conformational control of Pyr4 (Scheme 1B). Their structures were determined by 1D and 2D NMR analyses, and further confirmed by the recently developed crystalline sponge (CS) method which enables 'crystal-free' X-ray crystallography.[21]

We were also interested in the flexibility of Pyr4 towards changes in the farnesyl chain and therefore subjected substrate analogues **9a/9b** and **10a/10b** to Pyr4. Indeed, Pyr4 was able to convert (10*S*,3'*R*)-**10a** to the new meroterpenoid **15** bearing a *cis*-fused B/C ring system, presumably derived from a chair-chair substrate conformation (Scheme 1C). The natural substrate of Pyr4 contains an (*S*)-configured epoxide functionality. Interestingly, all productive enzyme substrate combinations were restricted to the (10*S*)-series of substrates, as none of the analogous (10*R*)-epoxy substrates (10*R*)-**7b**, (10*R*)-**8b**,

(10*R*)-**9b** or (10*R*)-**10b** were accepted. This finding indicates a strict recognition of the epoxide within the substrate binding site of the enzyme.

In addition, we found that MacJ' can also produce products **13** and **14** from (10*S*)-**8a** and **15** from (10*S*,3'*R*)-**10a** (Scheme 1B/C). MacJ, naturally involved in the biosynthesis of the drimane meroterpenoid macrophorin A, is one of the few known Pyr4-like cyclases which do not require substrate activation by epoxidation. Instead, MacJ is able to directly protonate the terminal double bond to initiate cyclization (Figure 2, Figure S6A). It is therefore interesting to note that MacJ also exhibits a clear preference for the (10*S*)-stereoisomers of epoxide substrates evaluated (Table 1, Figure S2-5).

Substrate Scope of CdmG and AscF

A meroterpenoid cyclase which is phylogenetically closely related to Pyr4 is CdmG (Figure 2), utilized in the biosynthetic pathway towards chrodrimanins from *Penicillium verruculosum*.[12] Chrodrimanins exhibit strong inhibitory activities against protein tyrosine phosphatase 1B (PTP1B) and are potential drug candidates for the treatment of type 2 diabetes and obesity.[22] CdmG naturally catalyzes the formation of 3-hydroxypentacecilide A (**17**) from (*S*)-configured epoxide **16**. In contrast to Pyr4, CdmG controls the substrate conformation in a chair-boat manner, leading to an inverted stereochemical outcome for the *trans*-configured B/C ring system (Scheme 2A). With this apparent change in conformational control, we were interested in determining the substrate promiscuity of CdmG and the putative differences in product formation.

When CdmG was incubated with synthetic substrates, a high degree of promiscuity was also observed as **7a**, **8a**, **9a**, and **10a** were accepted by CdmG and led to the production of new products (Figure S2-S5, Table 1). Whereas products from substrate (10*S*)-**7a** were found to be too unstable for structural characterization, products from substrates **8a**, **9a**, and **10a** were successfully isolated and structurally characterized. Reaction with (2*E*,6*E*)-configured substrate (10*S*)-**8a** led to formation of compound **18**, the 8,*9*-epimer of **13**, derived from the (10*S*,3'*S*)-**8a** isomer. The structure of **18** was determined by 2D NMR analysis and was further supported by X-ray-CS-diffraction data. The stereochemical outcome of the cyclization indeed demonstrated a conserved chair-boat conformational control of the substrate by the enzyme (Scheme 2B).

Reaction of CdmG with (10*S*)-**9a** represents the only case where two products were found derived from one substrate stereoisomer, in this case (10S,5'S)-**9a**, leading to the isolation of **19** and **20**. Whereas **19** is produced from a C-O bond forming event, product **20** is derived from C-C bond formation. In both cases, the same *trans-cis* configuration is observed for the A/B/C-ring system (Scheme 2C). Compounds **19** and **20** have also recently been identified from chemical cyclization where it was further shown that **20** can be rearranged to **19** by formic acid treatment.[11] To confirm the enzymatic origin of **19**, **20** was incubated under enzyme reaction conditions (KPP pH 7.4, 16 h, 30°C) but was found to not interconvert to **19**.

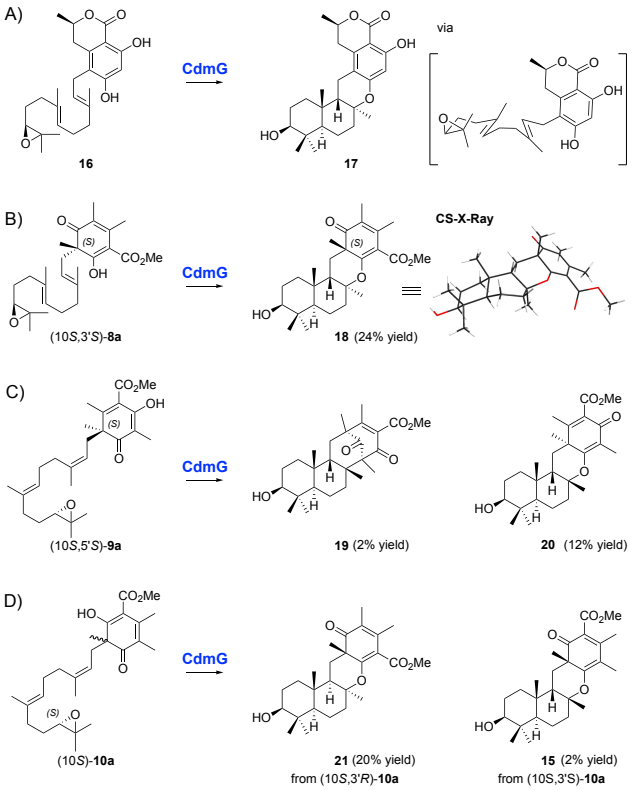

Scheme 2. A) Natural Reaction of CdmG and isolated meroterpenoids obtained from CdmG-mediated reactions with B) (10*S*,3'*S*)-**8a**; C) (10*S*,5'*S*)-**9a**; D) (10*S*)-**10a**.

Reaction of CdmG with (2*Z*,6*E*)-configured substrate **10a** produced the new meroterpenoids **15** and **21** (3:1) derived from a chair-boat substrate conformation (major) and a chair-chair substrate conformation (minor), respectively. As observed for the promiscuity of Pyr4, CdmG also had a strict preference for the epoxide stereoconfiguration, as none of the (10*R*)-epoxides were accepted by CdmG.

AscF from the ascochlorin pathway (Figure S6B) was found to also produce **21** from (10*S*)-**10a** as the only accepted substrate (Table 1, Figure S2-S5) and thus represents a meroterpenoid cyclase with very low tolerance towards alternative substrates.

Substrate Scope of AndB

The meroterpenoid cyclase AndB (Figure 2) from the andiotomin pathway[13] utilizes DMOA-derived substrate **22** with an (*S*)-configured epoxide to produce preandiloid A (**23**) with chair-boat conformation. In contrast to the results discussed for CdmG, which also controls the conformation in a chair-boat manner, AndB was found to exhibit a differing selectivity based on the stereocenter at the 3'- and 5'-stereocenters and therefore was found to produce different products (Table 1, Figure S2-S5). Specifically, AndB was found to accept (10*S*,3'*R*)-**8a** to produce the novel meroterpenoid **24** (Scheme 3). Similar to CdmG and Pyr4, the native conformational control of the prenyl chain was conserved, as a chair-boat substrate arrangement was found leading to **24**. AndB also accepted the (2*Z*,6*E*)-configured substrate (10*S*,5'*R*)-**9a** leading to the isolation of meroterpenoid **25**. The structure elucidation for **25** was challenging as 2D NMR analysis did not clearly reveal the

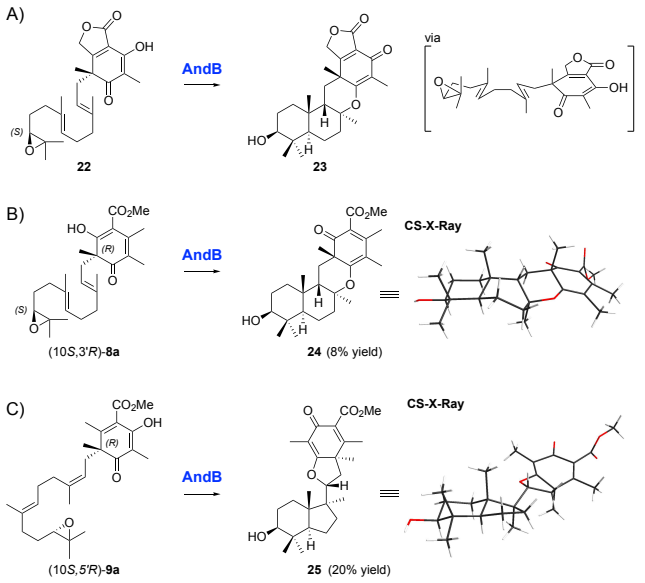

Scheme 3. A) Natural reaction of AndB and structures of isolated meroterpenoids obtained from AndB-mediated reactions with B) (10*S*,3'*R*)-**8a**; C) (10*S*,5'*R*)-**9a**.

connectivity between the terpenoid and non-terpenoid portions. Additionally, the relative configuration between the A/B and C/D ring systems were difficult to determine due to ambiguous NOESY correlations. However, we were able to fully establish the structure of **25** using crystalline sponge-X-ray analysis which revealed the presence of an unprecedented 6-5-ring system connected to a 5-6 ring system *via* a single C-C bond (Scheme 3C).

DFT Calculations for the Formation of 25, 20, CC and 19

The latter finding was surprising, as all reactions in this study lead to the formation of 6-6-ring systems for the A/B rings and also no natural cyclization towards 6-5-ring systems has been reported thus far. To gain further insight into the cyclization mechanism for the formation of **25** from (10*S*,5*R*)-**9a** by AndB, we conducted computational studies using density functional theory (DFT) at the B3LYP-D3(BJ)/6-31G(d,p)//B3LYP/6-31G(d,p) and CPCM(H_2O)-B3LYP-D3(BJ)/6-31G(d,p)//B3LYP/6-31G(d,p) levels[23] (see SI for details). The results (Figure 4) revealed that the first intermediate in the reaction cascade (modelled here in the absence of enzyme) is the monocyclic tertiary cation **A**, generated by an endergonic process *via* transition state **9a-TS**. **A** is then converted, after a conformational change, to **25**-H+ by an exergonic concerted process consisting of formation of the 5-membered B-ring in tandem with nucleophilic attack of the adjacent oxygen functionality via transition state **A-TS**. Inclusion of implicit solvent (CPCM(H_2O), in parentheses; single point calculations on previously optimized geometries in gas phase) led to lower barriers (Figure 4).[24],[25] With either a nonpolar (gas phase) or polar (water) surroundings, the barrier for initial cyclization is high for a biological reaction,[26] however, in the absence of enzyme, reactant (10*S*,5*R*)-**9a**-H+ relaxes to a non-productive conformation with an internal hydrogen-bond between the alcohol and epoxide; consequently, conformational preorganization by the enzyme should lower the barrier and this could be assisted by specific oriented noncovalent interactions with the transition state structure. An alternative mechanism for formation of the second ring could involve Markovnikov addition to form a 6-6 intermediate, followed by ring-contraction in concert with tetrahydrofuran ring formation. We find, however, that Markovnikov addition leads directly to a "6-6-6-6" product (**C**) that is not experimentally observed. We were able to optimize tertiary carbocation **B** as a minimum and this species can then undergo ring contraction to yield **25**-H+, but accessing **B** would require escape from the deep energy well associated with **C** and a large conformational change. The enzyme would, however, have to distinguish between **A-TS** and **A'-TS**, again by conformational biasing and/or well-placed noncovalent interactions with the transition state structure.

Formation mechanisms for **20** and **CC** from protonated stereoisomers of **9a** were also subjected to computational analysis. For both reactions (Figures 5A and B), we find highly asynchronous but concerted pathways in which no discrete carbocationic intermediates are formed. Similar concerted polycyclizations have been reported for related systems.[27] Both reactions also are predicted to be essentially barrierless once productive reactant conformations are attained, suggesting that preorganization controls which product is formed by a given enzyme. Conversion of **20**-H+ to **19**-H+ is predicted to be an endergonic process (Figure 6; neutral**19**is predicted to be several kcal/mol lower in energy than neutral **20**, however[11]), but an appropriately positioned base in a restricted enzyme active could selectively deprotonate **19**-H+. The barrier for the **20**-H+ to **19**-H+ interconversion is also less certain than others described above, since this reaction involves asynchronous bond-breaking, C–C bond rotation, and bond-making that leads to a "loose" transition state for which entropy and the effects of externally-imposed conformational constraints are difficult to estimate.

Substrate scope of Trt1, AdrI', PrhH, and NvfL

Another phylogenetic clade is formed by Trt1, AdrI, AdrI', AusL, and PrhH (Figure 2). These enzymes share the DMOA substrate (10*R*,5'*R*)-**7b**, but differ with regard to their product specificity. Trt1 catalyzes the formation of preterretonin (**27**) *via* a chair-chair-chair substrate conformation forming intermediary cation **26**, followed by Wagner-Meerwein rearrangement and a terminating deprotonation of H_a. AdrI shares the intermediary cation **26** and rearrangement, but differs in the terminating deprotonation side (H_b) producing andrastin E (**28**). AusL and PrhH both catalyze the formation of protoaustinoid A (**29**) from **26** after direct deprotonation of H_c (Scheme 4A). NvfL from the novofumigatonin pathway utilizes a highly similar substrate as Trt1, AdrI, AusL, and PrhH, carrying a free carboxylic acid instead of the methyl ester in the DMOA-unit. The free acid is crucial for enzyme function and the protein catalyzes formation of a spiro-center (Figure S6C). Consistent with the obvious tight recognition of the polyketide portion necessary to achieve these sophisticated and distinct reactions, a comparable low promiscuity for this group of integral membrane-bound enzymes was observed. Whereas PrhH and NvfL did not accept any of the tested unnatural substrates, both Trt1 and AdrI' accepted (2*Z*,6*E*)-**9b**, with the natural 5'-substitution

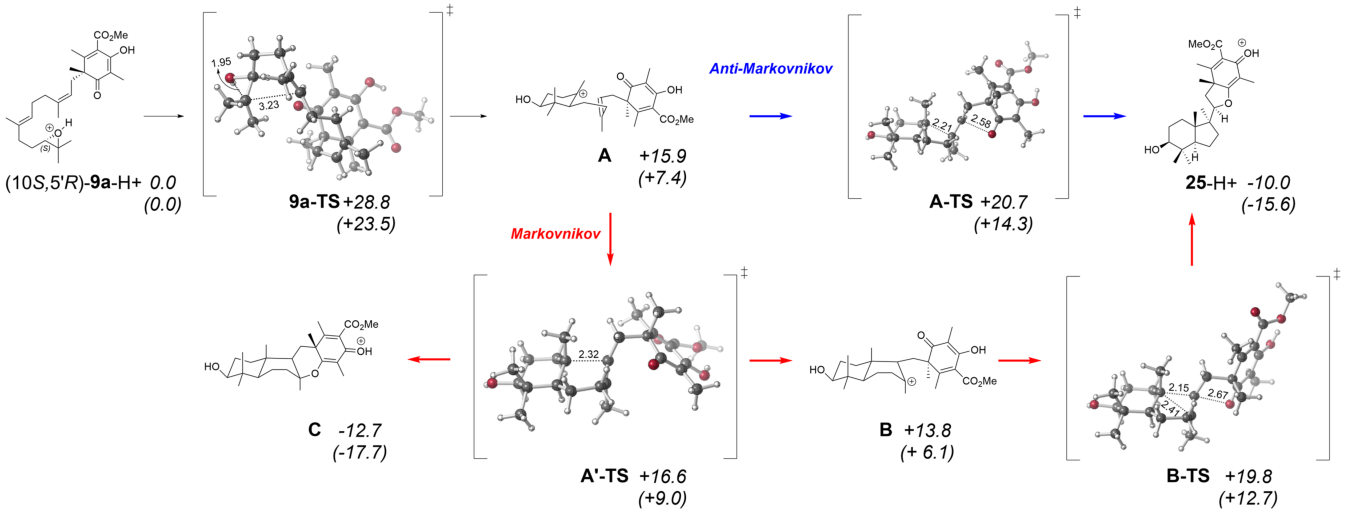

Figure 4. DFT calculations for the cyclization mechanism of (10*S*,5'*R*)-**9a** towards **25** by AndB. Two conformers of **A** were located, one connected to **9a-TS** and another connected to **A-TS**, which differ in energy by 0-3 kcal/mol, depending on the level of theory; see SI for details. Computed (B3LYP-D3(BJ)/6-31G(d,p)//B3LYP/6-31G(d,p) in black (top), CPCM(H_2O)-B3LYP-D3(BJ)/6-31G(d,p)//B3LYP/6-31G(d,p) in parentheses (bottom)) relative free energies (kcal/mol, *italics*) for minima and transition state structures (TSSs) involved in formation of compound 25. Bond distances are in Angstroms (Å).

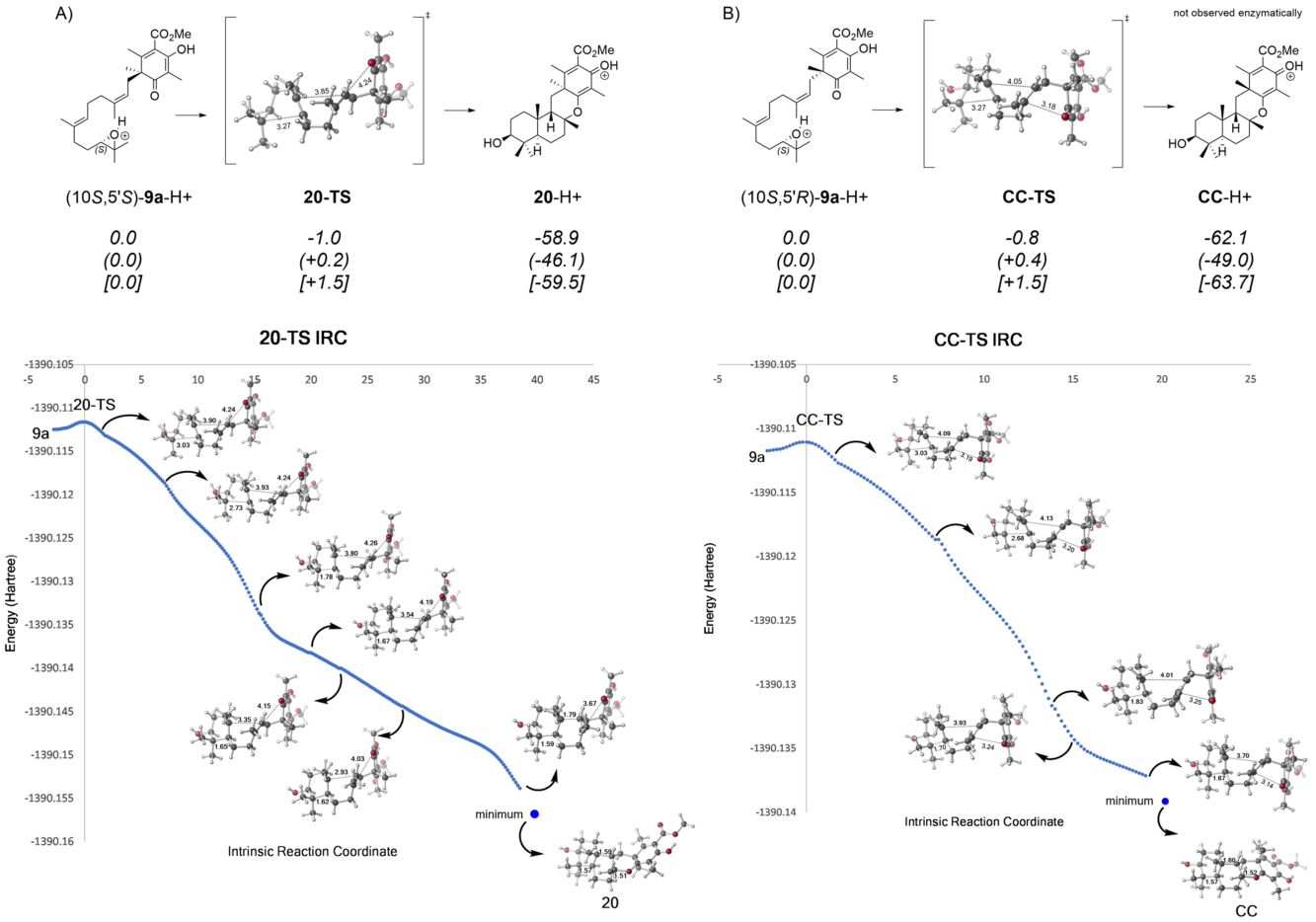

Figure 5. DFT calculations for the cyclization mechanism for the formation of A) **20** and B) **CC.** Computed (B3LYP-D3(BJ)/6-31G(d,p)//B3LYP/6-31G(d,p) (on top), CPCM(H_2O)-B3LYP-D3(BJ)/6-31G(d,p)//B3LYP/6-31G(d,p) (in parentheses) and MPW1PW91/6-31G(d,p)//B3LYP/6-31G(d,p) [in brackets]) relative free energies (kcal/mol, *italics*) for minima and transition state structures (TSSs) and IRC traces for the respective TSSs. Bond distances are in Angstroms (Å).

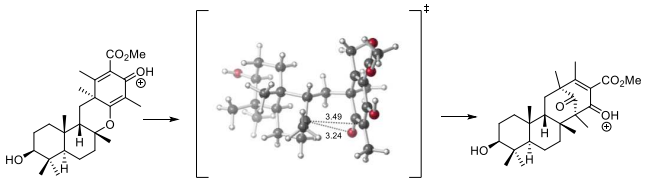

Figure 6. DFT calculations for the interconversion of **20**-H+ to **19**-H+. Computed (B3LYP-D3(BJ)/6-31G(d,p)//B3LYP/6-31G(d,p) (on top), CPCM(H_2O)-B3LYP-D3(BJ)/6-31G(d,p)//B3LYP/6-31G(d,p) (in parentheses) and MPW1PW91/6-31G(d,p)//B3LYP/6-31G(d,p) [in brackets]) relative free energies (kcal/mol, ***italics***) for minima and transition state structures (TSSs). Bond distances are in Angstroms (Å).

pattern in the polyketide portion (Table 1, Figure S2-S5).

However, for these cases products were found to be too unstable for structure determination. To our surprise, we found that Trt1 as well as AdrI' were able to convert (10*S*)-**7a**, the native substrate with inverted stereochemistry with respect to the epoxide functionality. We succeeded in the isolation of the Trt1-mediated product from (10*S*,5'*R*)-**7a** and the structure was determined to be 3-*epi*-preterretonin (**30**). The formation of this product can be envisioned to occur *via* a boat-chair substrate conformation (Scheme 4B).[28]

Enzyme Kinetics of Trt1

To shed additional light on the substrate promiscuity of meroterpenoid cyclases, we were interested in the comparison of the K_M values of the natural substrate to unnatural substrate analogous. Synthetic (10*R*,5'*R*)-**7b** is the natural substrate of Trt1, which was also found to accept unnatural (10*S*,5'*R*)-**7a**, and (10*R*)-**9b**. Since Trt1 and other meroterpenoid cyclases cannot be purified, the integral membrane bound enzyme was used as a crude enzyme preparation. To ensure a comparable enzyme concentration, Trt1 was freshly prepared and used for all kinetic assays on the same day. The results revealed an apparent K_M value of 34 μM for the natural substrate **7b**, whereas a 3-fold (95 μM) and 5-fold (144 μM) higher value was found for substrates **7a** and **9b**, respectively. The V_{max} values were determined as 22 μM/min, 7 μM/min and 0.5 μM/min, for **7b**, **7a** and **9b**, respectively. These findings indicate that the unnatural substrates have a lower affinity for the enzyme, but the values are of the same order of magnitude and thus further demonstrate the promiscuity observed for this enzyme class.

Summary and Conclusion

In summary, we have demonstrated chemoenzymatic access to twelve complex, unnatural DMOA-derived meroterpenoids of which eight represent novel compounds

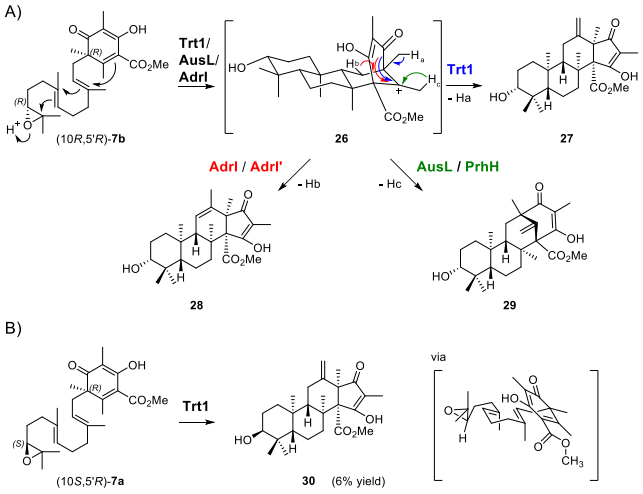

Scheme 4. A) Natural reaction of Trt1, AdrI/AdrI' and AusL/PrhH. B) Isolated meroterpenoids obtained from Trt1-mediated reactions with (10*S*,5'*R*)-**7a**.

by exploiting the surprisingly high promiscuity of fungal meroterpenoid cyclases.

Synthetic 3,5-dimethylorsellinic acid (DMOA)-containing substrates were prepared using dearomative alkylation and evaluated against nine meroterpenoid cyclases. The results demonstrate tight recognition of the epoxide functionality by the cyclase panel, but tolerance towards the polyketide portion. The conserved cyclization mechanism initiated by epoxide protonation and rigid control of the substrate conformation in the cyclase active site cavity led to the formation of several variations of naturally occurring meroterpenoid scaffolds, as well as generation of a completely new scaffold, although the number of cyclization steps that are concatenated into concerted processes appears to be system-dependent. The challenging structure elucidation and determination of relative and absolute configurations for the obtained enzyme products was solved by combining 2D NMR data analysis with the recently developed method of crystalline-sponge-X-ray diffraction analysis. This method allowed us to access the crystallographic data of non-crystalline enzyme products such as **25** for unambiguous structure determination and thus represents a powerful technique in combination with second generation natural product discovery.

The knowledge obtained in this study can be used for the design of artificial pathways by recombining biosynthetic genes in a suitable heterologous production host. Whereas productive enzyme combinations with naturally occurring substrates such as **7a** and **7b** provide a straightforward access by reconstituting known pathways towards these substrates and interchanging the introduced meroterpenoid cyclase, access to (2*Z*,6*E*)-configured prenyl substrates require further engineering efforts, for example, by employing a known bacterial (2*Z*,6*E*)-selective FPP synthase from *Mycobacterium*[29] and optimization of downstream enzymes towards substrates like **9a** and **9b**. Furthermore, the new meroterpenoids obtained can be evaluated as substrates for downstream tailoring enzymes such as α-ketoglutarate-dependent dioxygenases. Since several protein crystal structures have been reported in recent

years, protein engineering by either rational strategies or directed evolution represents an exciting opportunity to create novel "unnatural" meroterpenoids with valuable biological properties.[30]

ASSOCIATED CONTENT

Supporting Information. The Supporting Information, containing supplementary figures, materials and methods, experimental procedures, compound characterization, computational studies, additional references, and NMR spectra. This material is available free of charge via the Internet at http://pubs.acs.org.

AUTHOR INFORMATION

Corresponding Author

*abei@mol.f.u-tokyo.ac.jp
*porco@bu.edu
*djtantillo@ucdavis.edu

Author Contributions

‡T. Mitsuhashi, L. Barra, Z. Powers and V. Kojasoy contributed equally.

ACKNOWLEDGMENT

We thank the National Institutes of Health (R35 GM-118173, J. A. P., Jr.), a Grant-in-Aid for Scientific Research from the Ministry of Education, Culture, Sports, Science and Technology, Japan (JSPS KAKENHI Grant Number JP16H06443 and JP20H00490 to I.A.; JP19H05461 to M. F.), and the MEXT Nanotechnology Platform Program (Molecule and Material Synthesis) promoted at IMS for research funding. We also thank the Deutsche Forschungsgemeinschaft (DFG BA 6870/1-1) for a postdoctoral research fellowship to L.B. Computational work was supported by the National Science Foundation (CHE-1856416 and supercomputing resources from the XSEDE program via CHE-030089).

REFERENCES

(1) a) Cornforth, J. W. Terpenoid Biosynthesis. *Chem. Br.* **1968**, *4*, 102–106. b) Geris, R.; Simpson, T. J. Meroterpenoids Produced by Fungi. *Nat. Prod. Rep.* **2009**, *26* (8), 1063–1094. c) Kaysser, L.; Bernhardt, P.; Nam, S. J.; Loesgen, S.; Ruby, J. G.; Skewes-Cox, P.; Jensen, P. R.; Fenical, W.; Moore, B. S. Merochlorins A-D, Cyclic Meroterpenoid Antibiotics Biosynthesized in Divergent Pathways with Vanadium-Dependent Chloroperoxidases. *J. Am. Chem. Soc.* **2012**, *134* (29), 11988–11991. d) Peng, X.; Qiu, M. Meroterpenoids from Ganoderma Species: A Review of Last Five Years. *Nat. Prod. Bioprospect*. **2018**, *8* (3), 137–149.

(2) a) Ōmura, S.; Tomoda, H.; Kim, Y. K.; Nishida, H. Pyripyropenes, Highly Potent Inhibitors of Acyl-CoA: Cholesterol Acyltransferase Produced by *Aspergillus fumigatus*. *J. Antibiot.* **1993**, *46* (7), 1168–1169. b) Tomoda, H.; Kim, Y. K.; Nishida, H.; Masuma, R.; Ômura, S. Pyripyropenes, Novel Inhibitors of Acyl-CoA: Cholesterol Acyltransferase Produced by Aspergillus Fumigatus. I. Production, Isolation, and Biological Properties. *J. Antibiot. (Tokyo).* **1994**, *47* (2), 148–153. c) Das, A.; Davis, M. A.; Tomoda, H.; Ōmura, S.; Rudel, L. L. Identification of the Interaction Site within Acyl-CoA:Cholesterol Acyltransferase 2 for the Isoform-Specific Inhibitor Pyripyropene A. *J. Biol. Chem.* **2008**, *283* (16), 10453–10460.

(3) a) Horikoshi, R.; Goto, K.; Mitomi, M.; Oyama, K.; Sunazuka, T.; Ōmura, S. Identification of Pyripyropene A as a Promising Insecticidal Compound in a Microbial Metabolite Screening. *J. Antibiot.* **2017**, *70* (3), 272–276. b) Dieleman, C.; Knieriem, T.; Krapp, M.; Kierkus, P. C.; Xu, W.; Benton, K. Composition Containing a Pyripyropene Insecticide and a Base. Patent: *WO 2012/035010 A1*, **2012**.

(4) a) Sintchak, M. D.; Fleming, M. A.; Futer, O.; Raybuck, S. A.; Chambers, S. P.; Caron, P. R.; Murcko, M. A.; Wilson, K. P. Structure and Mechanism of Inosine Monophosphate Dehydrogenase in Complex with the Immunosuppressant Mycophenolic Acid. *Cell* **1996**, *85* (6), 921–930. b) Clutterbuck, P. W.; Oxford, A. E.; Raistrick, H.; Smith, G. Studies in the Biochemistry of Micro-Organisms: The Metabolic Products of the Penicillium Brevi-Compactum Series. *Biochem. J.* **1932**, *26* (5), 1441–1458. c) Canonica, L.; Kroszczynski, W.; Ranzi, B. M.; Rindone, B.; Santaniello E.; Scolastico, C. Biosynthesis of Mycophenolic Acid. *J. Chem. Soc., Perkin Trans. 1.* **1972**, 2639–2643. d) Shaw, L. M.; Nowak, I. Mycophenolic Acid: Measurement and Relationship to Pharmacologic Effects. *Ther. Drug Monit.* **1995**, *17* (6), 685–689.

(5) a) Ōmura, S.; Inokoshi, J.; Uchida, R.; Shiomi, K.; Masuma, R.; Kawakubo, T.; Tanaka, H.; Iwai, Y.; Kosemura, S.; Yamamura, S. Andrastins A-C, New Protein Farnesyltransferase Inhibitors Produced by *Penicillium* sp. FO-3929: I. Producing Strain, Fermentation, Isolation, and Biological Activities. *J. Antibiot.* **1996**, *49* (5), 414–417. b) Uchida, R.; Shiomi, K.; Inokoshi, J.; Sunazuka, T.; Tanaka, H.; Iwai, Y.; Takayanagi, H.; Ōmura, S. Andrastins A-C, New Protein Farnesyltransferase Inhibitors Produced by *Penicillium* sp. FO-3929: II. Structure Elucidation and Biosynthesis. *J. Antibiot.* **1996**, *49* (5), 418–424.

(6) Cueto, M.; Macmillan, J. B.; Jensen, P. R.; Fenical, W. Tropolactones A – D, Four Meroterpenoids from a Marine-Derived Fungus of the Genus *Aspergillus*. *Phytochemistry* **2006**, *67* (16), 1826–1831.

(7) Itoh, T.; Tokunaga, K.; Matsuda, Y.; Fujii, I.; Abe, I.; Ebizuka, Y.; Kushiro, T. Reconstitution of a Fungal Meroterpenoid Biosynthesis Reveals the Involvement of a Novel Family of Terpene Cyclases. *Nat. Chem.* **2010**, *2* (10), 858–864.

(8) a) Matsuda, Y.; Abe, I. Biosynthesis of Fungal Meroterpenoids. *Nat. Prod. Rep.* **2016**, *33* (1), 26–53. b) Matsuda, Y.; Awakawa, T.; Mori, T.; Abe, I. Unusual Chemistries in Fungal Meroterpenoid Biosynthesis. *Curr. Opin. Chem. Biol.* **2016**, *31*, 1–7.

(9) Rudolf, J. D.; Chang, C. Y. Terpene Synthases in Disguise: Enzymology, Structure, and Opportunities of Non-Canonical Terpene Synthases. *Nat. Prod. Rep.* **2020**, *37* (3), 425–463.

(10) a) Young, C. A.; Bryant, M. K.; Christensen, M. J.; Tapper, B. A.; Bryan, G. T.; Scott, B. Molecular Cloning and Genetic Analysis of a Symbiosis-Expressed Gene Cluster for Lolitrem Biosynthesis from a Mutualistic Endophyte of Perennial Ryegrass. *Mol. Genet. Genomics* **2005**, *274* (1), 13–29. b) Nicholson, M. J.; Koulman, A.; Monahan, B. J.; Pritchard, B. L.; Payne, G. A.; Scott, B. Identification of Two Aflatrem Biosynthesis Gene Loci in *Aspergillus flavus* and Metabolic Engineering of *Penicillium paxilli* to Elucidate Their Function. *Appl. Environ. Microbiol.* **2009**, *75* (23), 7469–7481. c) Tagami, K.; Liu, C.; Minami, A.; Noike, M.; Isaka, T.; Fueki, S.; Shichijo, Y.; Toshima, H.; Gomi, K.; Dairi, T.; Oikawa, H. Reconstitution of Biosynthetic Machinery for Indole-Diterpene Paxilline in *Aspergillus oryzae*. *J. Am. Chem. Soc.* **2013**, *135* (4), 1260–1263. d) Kato, H.; Tsunematsu, Y.; Yamamoto, T.; Namiki, T.; Kishimoto, S.; Noguchi, H.; Watanabe, K. New Natural Products Isolated from *Metarhizium robertsii* ARSEF 23 by Chemical Screening and Identification of the Gene Cluster through Engineered Biosynthesis in *Aspergillus nidulans* A1145. *J. Antibiot.* **2016**, *69* (7), 561–566. e) Yao, T.; Liu, J.; Liu, Z.; Li, T.; Li, H.; Che, Q.; Zhu, T.; Li, D.; Gu, Q.; Li, W. Genome Mining of Cyclodipeptide Synthases Unravels Unusual TRNA-Dependent Diketopiperazine-Terpene Biosynthetic Machinery. *Nat. Commun.* **2018**, *9*, 4091. f) Tsukada, K.; Shinki, S.; Kaneko, A.; Murakami, K.; Irie, K.; Murai, M.; Miyoshi, H.; Dan, S.; Kawaji, K.; Hayashi, H.; Kodama, E. N.; Hori, A.; Salim, E.; Kuraishi, T.; Hirata, N.; Kanda, Y.; Asai, T. Synthetic Biology Based Construction of Biological Activity-Related Library of Fungal Decalin-Containing Diterpenoid Pyrones. *Nat. Commun.* **2020**, *11*, 1830. g) Li, H.; Sun, Y.; Zhang, Q.; Zhu, Y.; Li, S. M.;

Li, A.; Zhang, C. Elucidating the Cyclization Cascades in Xiamycin Biosynthesis by Substrate Synthesis and Enzyme Characterizations. *Org. Lett.* **2015**, *17* (2), 306–309. h) Yaegashi, J.; Romsdahl, J.; Chiang, Y. M.; Wang, C. C. C. Genome Mining and Molecular Characterization of the Biosynthetic Gene Cluster of a Diterpenic Meroterpenoid, 15-Deoxyoxalicine B, in *Penicillium canescens*. *Chem. Sci.* **2015**, *6* (11), 6537–6544.

(11) Powers, Z.; Scharf, A.; Cheng, A.; Yang, F.; Himmelbauer, M.; Mitsuhashi, T.; Barra, L.; Taniguchi, Y.; Kikuchi, T.; Fujita, M.; Abe, I.; Porco, J. A. Biomimetic Synthesis Biomimetic Synthesis of Meroterpenoids by Dearomatization-Driven Polycyclization. *Angew. Chem. Int. Ed.* **2019**, *58* (45), 16141–16146.

(12) Bai, T.; Quan, Z.; Zhai, R.; Awakawa, T.; Matsuda, Y.; Abe, I. Elucidation and Heterologous Reconstitution of Chrodrimanin B Biosynthesis. *Org. Lett.* **2018**, *20* (23), 7504–7508.

(13) a) Matsuda, Y.; Wakimoto, T.; Mori, T.; Awakawa, T.; Abe, I. Complete Biosynthetic Pathway of Anditomin: Nature's Sophisticated Synthetic Route to a Complex Fungal Meroterpenoid. *J. Am. Chem. Soc.* **2014**, *136* (43), 15326–15336. b) Nakashima, Y.; Mitsuhashi, T.; Matsuda, Y.; Senda, M.; Sato, H.; Yamazaki, M.; Uchiyama, M.; Senda, T.; Abe, I. Structural and Computational Bases for Dramatic Skeletal Rearrangement in Anditomin Biosynthesis. *J. Am. Chem. Soc.* **2018**, *140* (30), 9743–9750.

(14) a) Matsuda, Y.; Awakawa, T.; Abe, I. Reconstituted Biosynthesis of Fungal Meroterpenoid Andrastin A. *Tetrahedron* **2013**, *69* (38), 8199–8204. b) Matsuda, Y.; Quan, Z.; Mitsuhashi, T.; Li, C.; Abe, I. Cytochrome P450 for Citreohybridonol Synthesis: Oxidative Derivatization of the Andrastin Scaffold. *Org. Lett.* **2016**, *18* (2), 296–299.

(15) Matsuda, Y.; Bai, T.; Phippen, C. B. W.; Nødvig, C. S.; Kjærbølling, I.; Vesth, T. C.; Andersen, M. R.; Mortensen, U. H.; Gotfredsen, C. H.; Abe, I.; Larsen, T. O. Novofumigatonin Biosynthesis Involves a Non-Heme Iron-Dependent Endoperoxide Isomerase for Orthoester Formation. *Nat. Commun.* **2018**, *9*, 2587.

(16) a) Matsuda, Y.; Iwabuchi, T.; Fujimoto, T.; Awakawa, T.; Nakashima, Y.; Mori, T.; Zhang, H.; Hayashi, F.; Abe, I. Discovery of Key Dioxygenases That Diverged the Paraherquonin and Acetoxydehydroaustin Pathways in *Penicillium brasilianum*. *J. Am. Chem. Soc.* **2016**, *138* (38), 12671–12677. b) Zhang, T.; Wan, J.; Zhan, Z.; Bai, J.; Liu, B.; Hu, Y. Activation of an Unconventional Meroterpenoid Gene Cluster in *Neosartorya glabra* Leads to the Production of New Berkeleyacetals. *Acta Pharm. Sin. B* **2018**, *8* (3), 478–487.

(17) a) Itoh, T.; Tokunaga, K.; Radhakrishnan, E. K.; Fujii, I.; Abe, I.; Ebizuka, Y.; Kushiro, T. Identification of a Key Prenyltransferase Involved in Biosynthesis of the Most Abundant Fungal Meroterpenoids Derived from 3,5-Dimethylorsellinic Acid. *ChemBioChem* **2012**, *13* (8), 1132–1135. b) Matsuda, Y.; Awakawa, T.; Itoh, T.; Wakimoto, T.; Kushiro, T.; Fujii, I.; Ebizuka, Y.; Abe, I. Terretonin Biosynthesis Requires Methylation as Essential Step for Cyclization. *ChemBioChem* **2012**, *13* (12), 1738–1741. c) Guo, C. J.; Knox, B. P.; Chiang, Y. M.; Lo, H. C.; Sanchez, J. F.; Lee, K. H.; Oakley, B. R.; Bruno, K. S.; Wang, C. C. C. Molecular Genetic Characterization of a Cluster in *A. terreus* for Biosynthesis of the Meroterpenoid Terretonin. *Org. Lett.* **2012**, *14* (22), 5684–5687. d) Matsuda, Y.; Iwabuchi, T.; Wakimoto, T.; Awakawa, T.; Abe, I. Uncovering the Unusual D-Ring Construction in Terretonin Biosynthesis by Collaboration of a Multifunctional Cytochrome P450 and a Unique Isomerase. *J. Am. Chem. Soc.* **2015**, *137* (9), 3393–3401.

(18) a) Araki, Y.; Awakawa, T.; Matsuzaki, M.; Cho, R.; Matsuda, Y.; Hoshino, S.; Shinohara, Y.; Yamamoto, M.; Kido, Y.; Inaoka, D. K.; Nagamune, K.; Ito, K.; Abe, I.; Kita, K. Complete Biosynthetic Pathways of Ascofuranone and Ascochlorin in *Acremonium egyptiacum*. *Proc. Natl. Acad. Sci. U. S. A.* **2019**, *116* (17), 8269–8274. b) Quan, Z.; Awakawa, T.; Wang, D.; Hu, Y.; Abe, I. Multidomain P450 Epoxidase and a Terpene Cyclase from the Ascochlorin Biosynthetic Pathway in *Fusarium* sp. *Org. Lett.* **2019**, *21* (7), 2330–2334.

(19) Tang, M. C.; Cui, X.; He, X.; Ding, Z.; Zhu, T.; Tang, Y.; Li, D. Late-Stage Terpene Cyclization by an Integral Membrane Cyclase in the Biosynthesis of Isoprenoid Epoxycyclohexenone Natural Products. *Org. Lett.* **2017**, *19* (19), 5376–5379.

(20) Qi, C.; Bao, J.; Wang, J.; Zhu, H.; Xue, Y.; Wang, X.; Li, H.; Sun, W.; Gao, W.; Lai, Y.; Chen, J. G.; Zhang, Y. Asperterpenes A and B, Two Unprecedented Meroterpenoids from *Aspergillus terreus* with BACE1 Inhibitory Activities. *Chem. Sci.* **2016**, *7* (10), 6563–6572.

(21) a) Inokuma, Y.; Yoshioka, S.; Ariyoshi, J.; Arai, T.; Hitora, Y.; Takada, K.; Matsunaga, S.; Rissanen, K.; Fujita, M. X-Ray Analysis on the Nanogram to Microgram Scale Using Porous Complexes. *Nature* **2013**, *495* (7442), 461–466. b) Hoshino, M.; Khutia, A.; Xing, H.; Inokuma, Y.; Fujita, M. The Crystalline Sponge Method Updated. *IUCrJ* **2016**, *3* (2), 139–151.

(22) Yamazaki, H.; Nakayama, W.; Takahashi, O.; Kirikoshi, R.; Izumikawa, Y.; Iwasaki, K.; Toraiwa, K.; Ukai, K.; Rotinsulu, H.; Wewengkang, D. S.; Sumilat, D. A.; Mangindaan, R. E. P.; Namikoshi, M. Verruculides A and B, Two New Protein Tyrosine Phosphatase 1B Inhibitors from an Indonesian Ascidian-Derived *Penicillium verruculosum*. *Bioorganic Med. Chem. Lett.* **2015**, *25* (16), 3087–3090.

(23) a) Miehlich, B.; Savin, A.; Stoll, H.; Preuss, H. Results Obtained with the Correlation Energy Density Functionals of Becke and Lee, Yang and Parr. *Chem. Phys. Lett.* **1989**, *157* (3), 200‑206. b) Lee, C.; Yang, W.; Parr, G, R. Development of the Colic-Salvetti Correlation-Energy into a Functional of the Electron Density. *Am. Phys. Soc.* **1988**, *37* (2), 785‑789. c) Becke, A. D. Density-Functional Thermochemistry. III. The Role of Exact Exchange Perspective on Density Functional Theory Density-Functional Thermochemistry. III. The Role of Exact Exchange. *J. Chem. Phys.* **1993**, *98*, 4775. d) Grimme, S.; Ehrlich, S.; Goerigk, L. Effect of the Damping Function in Dispersion Corrected Density Functional Theory. *J. Comput. Chem.* **2011**, *32* (7), 1456‑1465. e) Takano, Y.; Houk, K. N. Benchmarking the Conductor-like Polarizable Continuum Model (CPCM) for Aqueous Solvation Free Energies of Neutral and Ionic Organic Molecules. *J. Chem. Theory Comput.* **2005**, *1* (1), 70‑77.

(24) We benchmarked our system using a variety of methods: CPCM(DCM)-B3LYP-D3(BJ)/6-31G(d,p)//B3LYP/6-31G(d,p), CPCM(MEOH)-B3LYP-D3(BJ)/6-31G(d,p)//B3LYP/6-31G(d,p), mPW1PW91/6-31G(d,p)//B3LYP/6-31G(d,p) and CPCM(MEOH)-mPW1PW91/6-31G(d,p)//B3LYP/6-31G(d,p). See SI for details. Matsuda, S. P. T.; Wilson, W. K.; Xiong, Q. Mechanistic Insights into Triterpene Synthesis from Quantum Mechanical Calculations. Detection of Systematic Errors in B3LYP Cyclization Energies. *Org. Biomol. Chem.* **2006**, *4* (3), 530‑543.

(25) **9a** is the conformer obtained from reverse **9a-TS** intrinsic reaction coordinate (IRC) analysis. **9a-TS** forward IRC product undergoes a conformational change to form **A** which is the reverse IRC product of **A-TS.** See SI for details. a) Gonzalez, C.; Schlegel, H. B. Reaction Path Following in Mass-Weighted Internal Coordinates. *J. Phys. Chem.* **1990**, *94* (14), 5523‑5527. b) Fukui, K. The Path of Chemical Reactions - the IRC Approach. *Acc. Chem. Res.* **1981**, *14* (12), 363‑368. c) Maeda, S.; Harabuchi, Y.; Ono, Y.; Taketsugu, T.; Morokuma, K. Intrinsic Reaction Coordinate: Calculation, Bifurcation, and Automated Search. *Int. J. Quantum Chem.* **2015**, *115* (5), 258‑269.

(26) Wang, S. C.; Tantillo, D. J. Theoretical Studies on Synthetic and Biosynthetic Oxidopyrylium-Alkene Cycloadditions: Pericyclic Pathways to Intricarene. *J. Org. Chem.* **2008**, *73* (4), 1516–1523.

(27) a) Tantillo, D. J. Recent Excursions to the Borderlands between the Realms of Concerted and Stepwise: Carbocation Cascades in Natural Products Biosynthesis. *J. Phys. Org. Chem.* **2008**, *21*, 561–570. b) Smentek, L.; Hess, B. A. Compelling Computational Evidence for the Concerted Cyclization of the ABC Rings of Hopene from Protonated Squalene. *J. Am. Chem. Soc.* **2010**, *132* (48), 17111–17117. c) McCulley, C.; Geier, M. J.; Hudson, B. M.; Gagne, M. R.; Tantillo, D. J. Biomimetic Platinum-Promoted Polyene Polycyclizations - Influence of Alkene

Substitution and Pre-Cyclization Conformations. *J. Am. Chem. Soc.* **2017**, *139*, 11158-11164.

(28) Abe, I.; Rohmer, M. Enzymic Cyclization of 2,3-Dihydrosqualene and Squalene 2,3-Epoxide by Squalene Cyclases: From Pentacyclic to Tetracyclic Triterpenes. *J. Chem. Soc. Perkin Trans. 1* **1994**, No. 7, 783–791.

(29) a) Schulbach, M. C.; Brennan, P. J.; Crick, D. C. Identification of a Short (C15) Chain *Z*-Isoprenyl Diphosphate Synthase and a Homologous Long (C50) Chain Isoprenyl Diphosphate Synthase in *Mycobacterium tuberculosis*. *J. Biol. Chem.* **2000**, *275* (30), 22876–22881. b) Schulbach, M. C.; Mahapatra, S.; Macchia, M.; Barontini, S.; Papi, C.; Minutolo, F.; Bertini, S.; Brennan, P. J.; Crick, D. C. Purification, Enzymatic Characterization, and Inhibition of the *Z*-Farnesyl Diphosphate Synthase from *Mycobacterium tuberculosis*. *J. Biol. Chem.* **2001**, *276* (15), 11624–11630.

(30) a) Nakashima, Y.; Mori, T.; Nakamura, H.; Awakawa, T.; Hoshino, S.; Senda, M.; Senda, T.; Abe, I. Structure Function and Engineering of Multifunctional Non-Heme Iron Dependent Oxygenases in Fungal Meroterpenoid Biosynthesis. *Nat. Commun.* **2018**, *9*, 104. b) Nakamura, H.; Matsuda, Y.; Abe, I. Unique Chemistry of Non-Heme Iron Enzymes in Fungal Biosynthetic Pathways. *Nat. Prod. Rep.* **2018**, *35* (7), 633–645.

Insert Table of Contents artwork here